

Geophysical Research Letters



RESEARCH LETTER

10.1029/2019GL083782

Key Points:

- First MMS observations of electric fields near reconnecting site in the magnetotail
- A newly devised measure of estimating proximity to the electron diffusion region
- Demonstration that when ions decouple the electron physics dominates

Correspondence to:

W. M. Macek,
macek@cbk.waw.pl

Citation:

Macek, W. M., Silveira, M. V. D., Sibeck, D. G., Giles, B. L., & Burch, J. L. (2019). *Magnetospheric Multiscale* Mission observations of reconnecting electric fields in the magnetotail on kinetic scales. *Geophysical Research Letters*, 46, 10.2955–10.302. <https://doi.org/10.1029/2019GL083782>






Received 24 MAY 2019

Accepted 24 JUL 2019

Accepted article online 2 AUG 2019

Published online 12 SEP 2019

Magnetospheric Multiscale Mission Observations of Reconnecting Electric Fields in the Magnetotail on Kinetic Scales

W. M. Macek^{1,2} , M. V. D. Silveira^{3,4} , D. G. Sibeck³ , B. L. Giles³ , and J. L. Burch⁵ 
¹Faculty of Mathematics and Natural Sciences, Cardinal Stefan Wyszyński University, Warsaw, Poland, ²Space Research Centre, Polish Academy of Sciences, Warsaw, Poland, ³NASA Goddard Space Flight Center, Greenbelt, MD, USA, ⁴Catholic University of America, Washington, DC, USA, ⁵Southwest Research Institute, San Antonio, TX, USA

Abstract We examine the role of ions and electrons in reconnection using the highest resolution observations from the *Magnetospheric Multiscale* mission on kinetic ion and electron scales. We report magnetic field and plasma observations from several approaches to the electron diffusion region in the current sheet in 2018. Besides magnetic field reversals, changes in the direction of flow velocity, ion and electron heating, *Magnetospheric Multiscale* observed large fluctuations in the electron flow speeds in the magnetotail. We have verified that when the field lines and plasma become decoupled, a large reconnecting electric field related to the Hall current (1–10 mV/m) is responsible for fast reconnection in the ion diffusion region. Although inertial acceleration forces remain moderate (1–2 mV/m), the electric fields resulting from the electron pressure tensor provide the main contribution to the generalized Ohm's law at the neutral sheet (as large as 200 mV/m). This illustrates that when ions decouple electron physics dominates.

Plain Language Summary We study the physical mechanism of magnetic reconnection. We use with unprecedented high time resolution (up to several milliseconds) *Magnetospheric Multiscale* plasma and magnetic field observations of magnetotail reconnection sites on ion and electron scales. We employ a newly devised method to estimate proximity to the electron diffusion region where ions decouple from electrons and electron physics dominates. The results obtained may also be useful for better understanding the physical mechanism governing reconnection processes in various magnetized laboratory and space plasmas.

1. Introduction

Reconnection is a complex phenomenon that remains a challenge for contemporary science. Notwithstanding great progress in magnetohydrodynamic (MHD; Hall-MHD, two-fluid) simulations, the physical mechanisms for reconnection are not clearly understood. Turbulent magnetic fields play an important role in space environments (Bruno & Carbone, 2016), leading to magnetic reconnection and the redistribution of kinetic and magnetic energy in space plasmas (Biskamp, 2000; Burlaga, 1995; Figura & Macek, 2013; Strumik et al., 2013; Strumik et al., 2014; Treumann, 2009; Treumann & Baumjohann, 2013; Vasyliunas, 1975). One of the main objectives of the *Magnetospheric Multiscale* (MMS) mission is to determine the role of turbulence in reconnection processes and the roles of ions and electrons in these processes.

Burch, Torbert, et al. (2016) report in situ evidence for a reconnection diffusion region at the dayside magnetopause using MMS measurements in a case study on 16 October 2016 that was further discussed by Torbert et al. (2016). A list of 32 such magnetopause events has been reported by Webster et al. (2018). Yordanova et al. (2016) reported observations of electron-scale structures and magnetic reconnection signatures in the turbulent magnetosheath using MMS measurements, while Øieroset et al. (2016) analyzed reconnection jets at the magnetopause. Wang et al. (2018) identified a current sheet on electron scales in the near-Earth magnetotail without bursty reconnection. By contrast, Torbert et al. (2018) studied a reconnection event on 11 July 2017. They reported that the spacecraft entered the electron diffusion region (EDR) in the magnetotail, suggesting that electron dynamics in this region was mostly laminar despite turbulence near the reconnection region. Daughton et al. (2014) reported a kinetic simulation of magnetopause

©2019. The Authors.

This is an open access article under the terms of the Creative Commons Attribution License, which permits use, distribution and reproduction in any medium, provided the original work is properly cited.

reconnection, while Nakamura et al. (2018) provided simulation results for a magnetotail case. Liu et al. (2019) have recently reported *MMS* observations of an electron-scale magnetic cavity embedded in a proton-scale cavity. One can hence expect that a detailed analysis of the high-resolution *MMS* data will provide significant insight into the nature of reconnection processes in space plasmas.

Note that during the magnetopause encounters of *MMS* in Phase 1, a rather large (1/3–1/2) residual component of the required reconnection electric field E_{rec} of a few millivolts per meter was absent (Torbert et al., 2016). In the case of magnetotail encounters with the EDR during Phase 2 (Torbert et al., 2018), the relative contributions of various terms in the generalized Ohm's law that contribute to anomalous resistivity has not been fully explored (Burch, Moore, et al., 2016).

This Letter focuses on the deviations from MHD, including Hall-MHD, electron pressure, and inertial effects on both ion and electron scales as seen in the *MMS* data, which warrants further investigation. Following our previous study of turbulence within highly variable plasmas using *MMS* data (Macek et al., 2018), we analyze in greater detail the electric fields on sub-ion scales in magnetotail regions near the *X* line, to compare the characteristics of reconnection processes when going from the ion to electron kinetic scales. This naturally leads to a description of space plasmas within kinetic theory, instead of the ideal MHD approach.

We find experimental evidence for somewhat turbulent (chaotic) reconnection in the magnetotail, as suggested by numerical simulations (Lazarian et al., 2015). We observe rather large reconnecting electric fields resulting from the Hall currents for plasma and magnetic field data of the highest resolution available within the *MMS* mission (Yamada et al., 2016). The additional components are caused by a moderate inertial term followed by the large pressure forces activated when approaching the reconnection site. Basically, the electric field related to the full electron pressure tensor becomes the main contribution showing that when ions decouple, the electron physics dominates, section 2. The ion and electron data are described in section 3. The reconnection electric and magnetic field data are presented in section 4. Finally, the importance of electron diffusion processes on sub-ion scales for astrophysical plasmas is summarized in section 5.

2. Methods

In two-fluid theory, the sum of all the contributions to the electric field, \mathbf{E}_{tot} , consisting of various terms, should be equal to the dissipation created by an anomalous resistivity η in the generalized Ohm's law. Basically, one should have (Rossi & Olbert, 1970)

$$\mathbf{E}_{\text{tot}} = \mathbf{E} + \mathbf{V} \times \mathbf{B} + \mathbf{E}_{\text{H}} + \mathbf{E}_{\text{a}} + \mathbf{E}_{\text{p}} = \eta \mathbf{j}, \quad (1)$$

with $\eta = \nu / \omega_{\text{pe}}^2$ (equivalent to collision frequency ν in ordinary fluids), where \mathbf{E}_{H} , \mathbf{E}_{a} , and \mathbf{E}_{p} denote the Hall, inertial, and pressure terms. Namely, the electric fields $E_{\text{rec}} = |\mathbf{V}_{\text{e}} \times \mathbf{B}_{\text{rec}}|$ responsible for dissipative processes at reconnection sites must be described by nonideal terms (Baumjohann & Treumann, 1996; Biskamp, 2000; Yamada et al., 2016) beyond the classical field $\mathbf{E}'_0 = \mathbf{E} + \mathbf{V} \times \mathbf{B} = \mathbf{R}$ seen in the rest frame by the plasma moving with the velocity \mathbf{V} , as well described by the ideal ($\mathbf{R} = 0$) MHD theory (Krall & Trivelpiece, 1973). Using the plasma density n (with quasineutrality $n_{\text{i}} = n_{\text{e}}$ and the electron to ion mass ratio $m_{\text{e}}/m_{\text{i}} \ll 1$), the bulk velocity of the plasma $\mathbf{V} = \mathbf{V}_{\text{i}} + (m_{\text{e}}/m_{\text{i}})\mathbf{V}_{\text{e}}/(1 + (m_{\text{e}}/m_{\text{i}}))$ is approximately equal to the velocity of the ions, $\mathbf{V} \approx \mathbf{V}_{\text{i}}$, provided that the velocities of the ions and electrons are of the same order of magnitude, $\mathbf{V}_{\text{i}} \sim \mathbf{V}_{\text{e}}$. However, in the presence of fast moving electrons generated by reconnection processes, this assumption may not always be satisfied. Therefore, MHD and Hall-MHD contributions to the electric field should be considered separately.

Inside the ion diffusion region (IDR), the main contribution to the electric field should come from the Hall term, $\mathbf{E}_{\text{H}} = -\mathbf{j} \times \mathbf{B}/(en)$, with the current density $\mathbf{j} = e(n_{\text{i}}\mathbf{V}_{\text{i}} - n_{\text{e}}\mathbf{V}_{\text{e}})$ (e is the electron elementary charge). Since $\mathbf{E}_{\text{H}} = (\mathbf{V}_{\text{e}} - \mathbf{V}_{\text{i}}) \times \mathbf{B}$ taking $\mathbf{V} \approx \mathbf{V}_{\text{i}}$ we have

$$\mathbf{E}' \equiv \mathbf{E}'_0 + \mathbf{E}_{\text{H}} = \mathbf{E} + \mathbf{V} \times \mathbf{B} + \mathbf{E}_{\text{H}} \approx \mathbf{E} + \mathbf{V}_{\text{e}} \times \mathbf{B}. \quad (2)$$

This means that electrons remain frozen and are convected by the magnetic field. It is worth noting that the Hall term is active on kinetic ion scales (Burch, Moore, et al., 2016). On the other hand, the new \mathbf{E}_{a} and \mathbf{E}_{p} terms describing the electric field resulting from the difference between accelerated electrons and ions and the thermal pressure of electrons relative to the ion background, respectively, should be important on both

ion and electron scales (Rossi & Olbert, 1970; Spitzer, 1956). Therefore, these two other inertial and thermal terms should also be important in the kinetic regime.

Namely, the first additional component to the nonideal electric field comes from the forces resulting during the acceleration of electrons (of mass m_e) and ions, $(e/m_e)\mathbf{E}_a = \left[\left(\frac{\partial}{\partial t} + \mathbf{V}_e \cdot \nabla \right) \mathbf{V}_e - \left(\frac{\partial}{\partial t} + \mathbf{V}_i \cdot \nabla \right) \mathbf{V}_i \right]$, turning electrons and ions from inflowing into outflowing current directions. Note that this is just the time and space change of the convective derivative of the electrons ($\frac{d}{dt} \equiv \frac{\partial}{\partial t} + \mathbf{V}_e \cdot \nabla$) and ion ($\frac{d}{dt} \equiv \frac{\partial}{\partial t} + \mathbf{V}_i \cdot \nabla$) jets moving rapidly from the X line, taken into consideration both the electron \mathbf{V}_e and ion \mathbf{V}_i flows. In the reconnection region, where forces resulting from separations of the accelerated electrons and ions should be taken into account, we have $e\mathbf{E}_a = m_e d(\mathbf{V}_e - \mathbf{V}_i)/dt$. Using the continuity conservation equations, $\frac{\partial n}{\partial t} + \nabla \cdot (n\mathbf{V}) = 0$, for both the ion and electron fluxes, one obtains the following formula:

$$\mathbf{E}_a = \frac{m_e}{e} \left\{ \frac{1}{n_e} \frac{\partial}{\partial t} (n_e \mathbf{V}_e) - \frac{1}{n_i} \frac{\partial}{\partial t} (n_i \mathbf{V}_i) \right\} + \frac{m_e}{e} \left\{ \frac{1}{n_e} \nabla \cdot [n_e (\mathbf{V}_e \cdot \mathbf{V}_e)] - \frac{1}{n_i} \nabla \cdot [n_i (\mathbf{V}_i \cdot \mathbf{V}_i)] \right\}, \quad (3)$$

corresponding to the conservation of the total anisotropic kinetic energy density flux in the stress tensor, which involves the divergence ∇ of this tensor (Landau et al., 1984). The partial time derivative in equation (3) describes the possibly unsteady component of the reconnection electric field, $-\frac{1}{\omega_{p,e}^2} \frac{\partial j}{\partial t}$, where $\omega_{p,e} = (n_e e^2 / m_e)^{1/2}$ is the electron plasma frequency, but we have verified that this contribution is small and can here be neglected.

The second (nonideal) contribution to the electric field results from the divergence of the fully anisotropic pressure (dyadic) tensor (Gurnett & Bhattacharjee, 2005), $\mathbf{P} \equiv m \int (\mathbf{V} - \mathbf{U})(\mathbf{V} - \mathbf{U}) f d^3\mathbf{V}$. Note that by averaging over velocity space for a given position $\mathbf{r} = (x, y, z)$ within an infinitesimally small fluid element of volume $d^3\mathbf{r} = dx dy dz$, one can write $\mathbf{P} = mn \langle (\mathbf{V} - \mathbf{U})(\mathbf{V} - \mathbf{U}) \rangle$ (Spitzer, 1956). This means that the pressure term should have a somewhat similar structure to that of the inertial term, the second component in equation (3), but with the distribution function f for individual particles moving randomly with velocities \mathbf{V} around the mean (bulk) velocity $\mathbf{U} \equiv \langle \mathbf{V} \rangle = \frac{1}{n} \int \mathbf{V} f d^3\mathbf{V}$ (approximately one has $\langle \mathbf{V} \rangle \simeq \frac{1}{\Delta N} \sum_{k=1}^{\Delta N} \mathbf{V}_k$, where $\Delta N \simeq n dx dy dz$). Because $m_e/m_i \ll 1$, the contribution from the ion pressure tensor can be neglected, and we only have the electron tensor electric field (Rossi & Olbert, 1970):

$$\mathbf{E}_p \equiv \frac{1}{en_e} \nabla \cdot \mathbf{P}_e = \frac{m_e}{en_e} \nabla \cdot [n_e \langle (\mathbf{V}_e - \mathbf{U})(\mathbf{V}_e - \mathbf{U}) \rangle], \quad (4)$$

where the diagonal thermal pressures are given by $p_{\parallel e} = n_e k T_{\parallel e}$ and $p_{\perp e} = n_e k T_{\perp e}$ parallel and perpendicular, respectively, with regard to the magnetic field \mathbf{B} , and k is Boltzmann constant, $T_{\parallel e} + 2T_{\perp e} = T \mathbf{T}_e$, including the off-diagonal components, are responsible for nongyrotropic (crescent) features of the electron distribution function f_e , and the temperature tensor $\mathbf{T}_e \equiv \mathbf{P}_e / (nk)$. The electric field given by equation (4) becomes important in the region where ions decouple and electron physics dominate. Hence, we propose that the ratio of the thermal pressure term in equation (4) to the sum of other terms including the ideal with Hall term \mathbf{E}' , equation (2), and the electron (inertial) accelerating \mathbf{E}_a contributions, equation (3), $r_e \equiv |\mathbf{E}_p| / |\mathbf{E}' + \mathbf{E}_a|$, to be a useful signature indicating approaches to the EDR.

3. Data

The *MMS* mission was launched in 2015 to investigate magnetic reconnection near the Earth's magnetopause and in the magnetotail (Burch, Moore, et al., 2016). This Letter investigates reconnection when crossing the current sheet in the magnetotail. Figure 1 shows *MMS* trajectories for the Cases 1–3 presented in Figures 2–4, respectively, in Geocentric Solar Magnetospheric (GSM) coordinates. Table 1 lists the respective time intervals with chosen characteristics (calculated when B_x changes sign): the measured current \mathbf{j} , the Hall electric field \mathbf{E}_H in the generalized Ohm's law, equation (1), the residual (anomalous) dissipation field $\mathbf{E}_{\text{tot}} = \eta \mathbf{j}$, and the energy density (power W) that should be dissipated by this (total) anomalous term including the parameter $r_e \equiv |\mathbf{E}_p| / |\mathbf{E}' + \mathbf{E}_a|$, postulated to be a signature indicating approaches to the site of the EDR.

For the magnetic field \mathbf{B} , we use burst-type observations from the fluxgate magnetometers (FGM) (Russell et al., 2016) with the highest cadence of 7.8 ms. The data are available online (<http://cdaweb.gsfc.nasa.gov>). For the ion and electron plasma velocities, \mathbf{V}_i and \mathbf{V}_e , we use observations from the Dual Ion and Electron Spectrometer (DIS, DES) instruments (Pollock et al., 2016), with somewhat lower time resolution: 150 ms sampling for ions and 30 ms for electrons, respectively. We consider an interesting interval lasting 8 s during

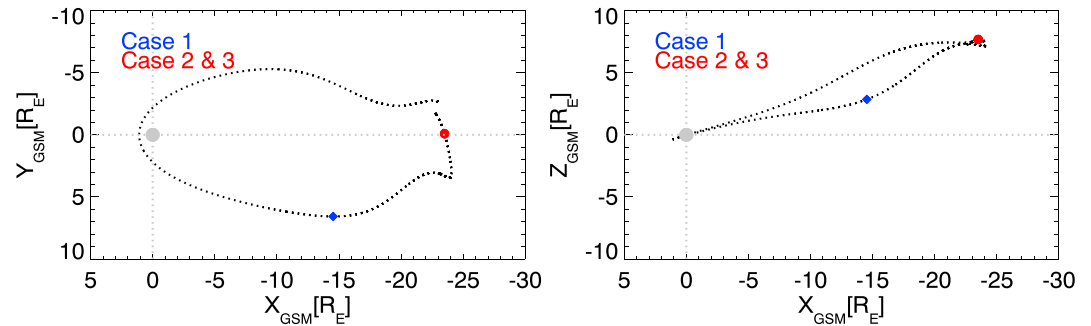


Figure 1. Magnetospheric Multiscale spacecraft trajectories and positions inside the magnetosphere near three crossings of the magnetotail 23 (Case 1) and 24 July 2018 (Case 2 and 3). GSM = Geocentric Solar Magnetospheric.

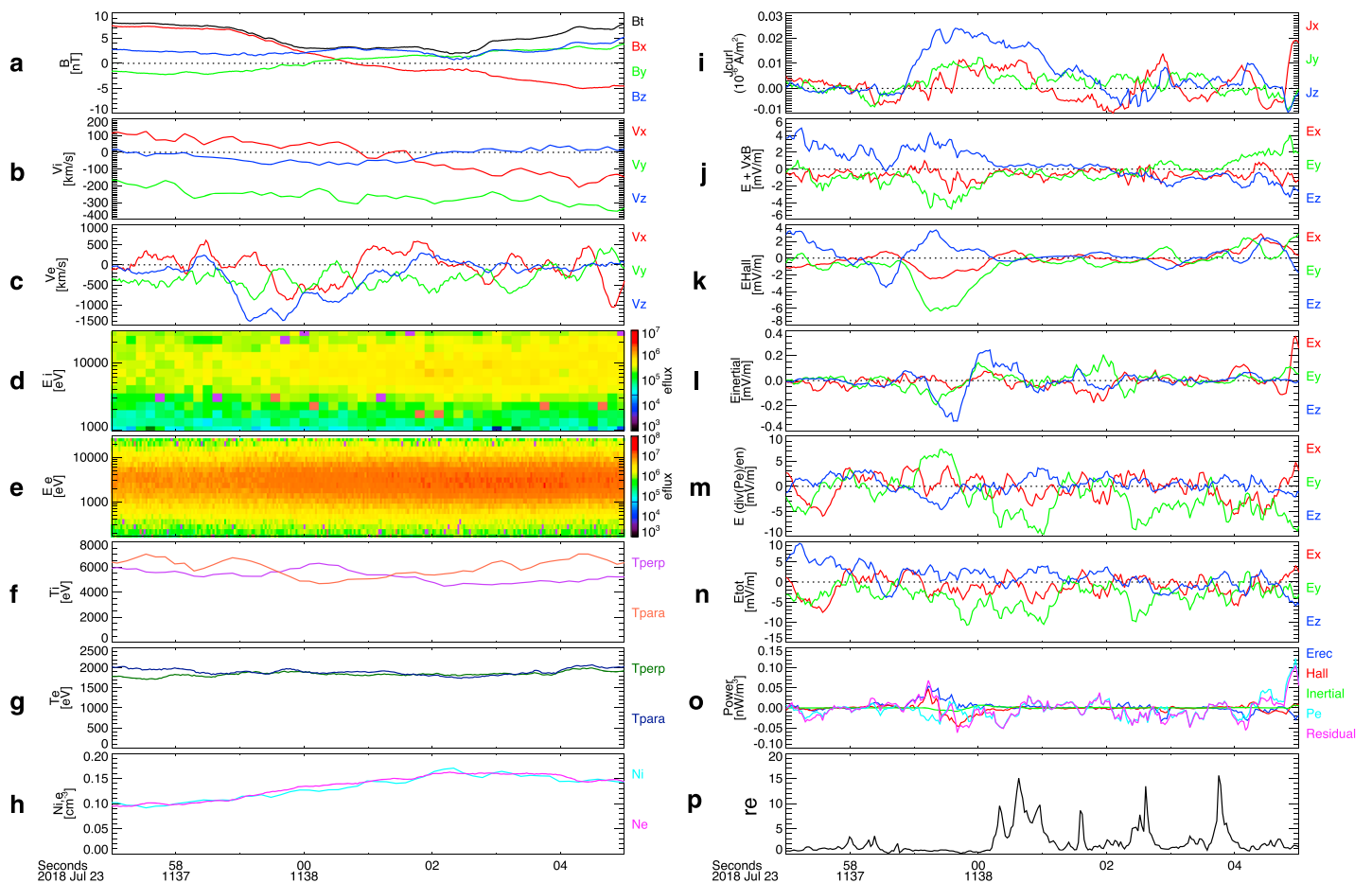


Figure 2. Data and derived electric field parameters identified by Magnetospheric Multiscale 2 spacecraft when crossing the magnetotail on 23 July 2018 centered at 11:38:01, Case 1 in Table 1: (a) magnetic field \mathbf{B} vector components, ion (b) and electron (c) velocity vectors, ion (d) and electron (e) energy spectra, and the ion (f) and electron (g) perpendicular T_{\perp} and parallel T_{\parallel} temperatures with density n_i and n_e (h); current \mathbf{j} (i) with derived electric field components contributions to the generalized Ohm's law: ideal $\mathbf{E} + \mathbf{V} \times \mathbf{B}$ (j), Hall \mathbf{E}_H (k), inertial acceleration \mathbf{E}_a (l), electron pressure \mathbf{E}_p (m), and residual (anomalous) η_j (n) terms. The electromagnetic energy density (power $W \sim \mathbf{j} \cdot \mathbf{E}$) is converted to plasma energy from various terms of \mathbf{E} (o) with the reconnection parameter r_e in (p).

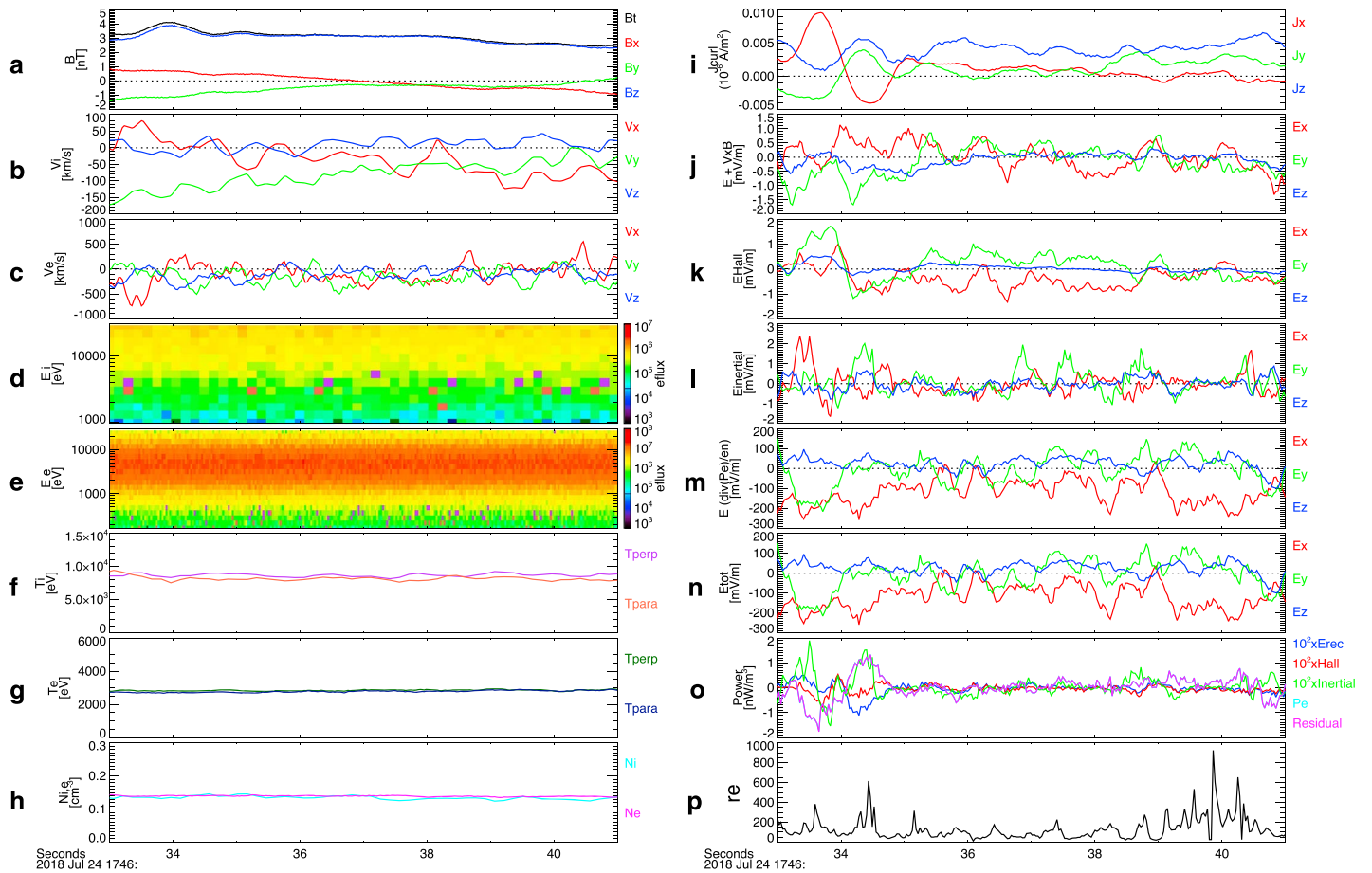


Figure 3. Data and electric fields identified by *Magnetospheric Multiscale 2* spacecraft when crossing the magnetotail on 24 July 2018 centered around 17:46:37, Case 2 in Table 1.

a magnetotail crossing on 23 July 2018 followed by two other events on the next day. Each interval studied comprises 1,026 points for the magnetic field \mathbf{B} and 267 (53) points for the ion and electron $\mathbf{V}_{i,e}$ velocity (Table 1).

4. Results

The left panels (panels a to h) of Figures 2–4 display the data used for the analysis. Because all probes observed similar structures, we display the data for only one spacecraft for each event. The *MMS2* magnetic field vector components including the magnitude are presented in panel a, with all components of the ion (b) and electron (c) velocity vectors, the ion (d) and electron (e) energy omnidirectional spectrograms, the ion (f) and electron (g) perpendicular T_{\perp} and parallel T_{\parallel} temperatures, and the ion and electron density n_i and n_e are shown in the panel h.

We see that the dominant component of the magnetic field, B_x , changes sign (at 11:38:01.22, 17:46:36.97, and 17:47:10.01) and the ion V_{ix} velocity changes sign nearly simultaneously, when crossing the current sheet, followed by distinct fast jets of electrons V_{ex} . Admittedly, in Figure 2, V_{ix} becomes zero, while V_{iy} is constantly negative with -300 km/s (this is a slight direction change in the downward flows), but B_z also change sign when approaching the reconnection site (Figure 4). Because densities are low in the magnetotail (0.10 – 0.15 cm $^{-3}$), we eliminate background noise from local spacecraft photoelectrons and residual penetrating radiation, by including only particles with energies greater than 165 eV for electrons and 975 eV for ions (panels e) in the respective partial distribution functions. Because the highest resolution available for the ion distributions is 5 times lower than that for electrons, we verified that the fluctuations in the electron speeds could be smoothed by using somewhat lower resolutions for electrons. A reversal in ion flow remains clear in panel b in Figures 2 and 3 and variations in electrons speeds also remain clear in panel

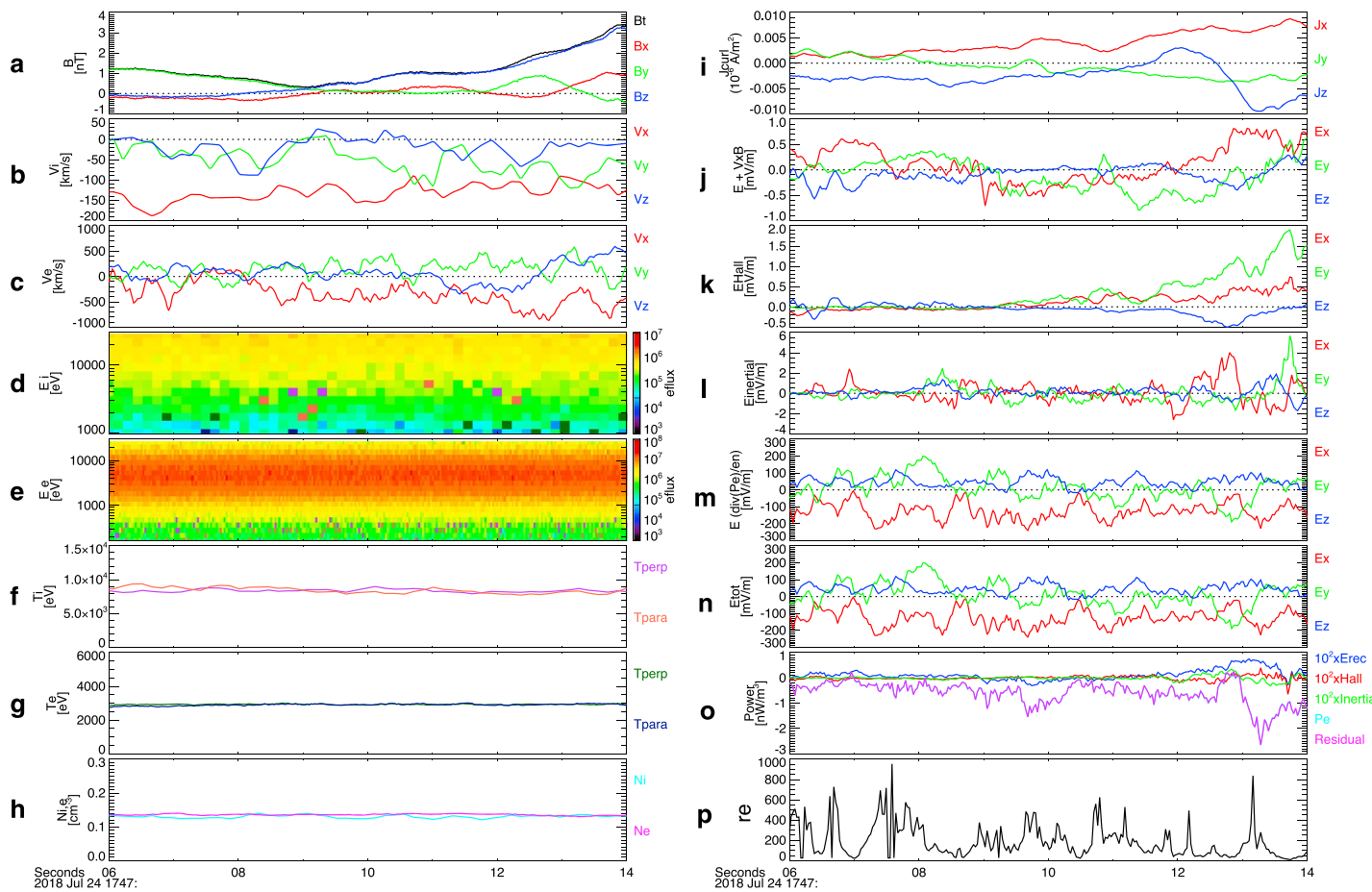


Figure 4. Data and electric fields identified by Magnetospheric Multiscale 2 spacecraft when crossing the magnetotail on 24 July 2018 centered around 17:47:10, Case 3 in Table 1.

c, smoothed by the same running averages of 0.3 s (twice the resolutions for ions, 0.15 s), consistent with quasineutrality achieved in panel h.

As compared with the case of 11 July 2017 when *MMS* crossed the EDR region (Torbert et al., 2018), large chaotic fluctuations in the electron velocities are present in the current sheet crossings in all 2018 events, which may exhibit some turbulent processes responsible for reconnection when approaching or passing by the *X* line. Besides the flow reversal, some heating is observed for both ions (up to energies of a few tens of kiloelectron volts) and electrons (1–10 keV) but compared with the temperature asymmetry observed in the EDR of 11 July 2017, for the current sheet crossing on 23 and 24 July 2018 roughly isotropic ion (3–6 keV) and electron temperatures (2–3 keV), are seen in panels d and e.

The main results of this paper with respect to the reconnecting electric fields are shown in the right panels from i to p of Figures 2–4. First, the current **j** obtained from the curl of the magnetic field **B** is displayed in panel i. The relatively large components during the crossing of the current sheet are seen in all the cases

Table 1

List of Selected Magnetospheric Multiscale Spacecraft (s-c) Interval Samples in the Magnetotail (hh:min:ss) With the Current **j** Observed at the Magnetic Field Reversal, the Hall Electric Field E_H in the Generalized Ohm's Law, the Residual (Anomalous) Dissipation Field $\eta \mathbf{j}$, the Power *W* Dissipated by the Anomalous Term, and the Parameter r_e Indicating Approaches to the Electron Diffusion Region

Case	s-c	Time (y.m.d)	Begin	End	\mathbf{j} ($\mu\text{A}/\text{m}^2$)	E_H (mV/m)	$\eta \mathbf{j}$	<i>W</i> (nW/m ³)	r_e
1	2	2018.07.23	11:37:57	11:38:05	0.0086	0.74	5.27	0.0088	1.5
2	1–3	2018.07.24	17:46:33	17:46:41	0.0373	0.25	117	−0.119	88.7
3	1–3	2018.07.24	17:47:06	17:47:14	0.0056	0.20	207	−0.994	207

shown. Besides the ideal field $\mathbf{E} + \mathbf{V} \times \mathbf{B}$ (of several millivolts per meter) seen in the frame of the plasma moving with the bulk speed \mathbf{V} (panel j), we display the nonideal electric fields resulting from the following terms: the Hall \mathbf{E}_H (panel k), inertial acceleration \mathbf{E}_a (l), and electron pressure \mathbf{E}_p (m) electric fields. The Hall electric fields of equation (2) were calculated using two methods, from the Ampere's law (curl of the magnetic field) and from the ion and electron data. This further validated the consistency of the calculations of moments of the electron distribution functions (only the curlometer current is shown in panel i).

It is interesting to compare the electric fields contributing to the generalized Ohm's law as displayed in panels j to m. We see that the electric field resulting from the Hall current is of the same order as the ideal field, and as expected, the Hall term still plays an important role for fast reconnection especially in the IDR. The contribution from the inertial term is rather small in Case 1 (a fraction of millivolts per meter) and moderate in Case 2 (about 1–2 mV/m) and Case 3. On the other hand, the large reconnection electric fields up to 10 mV/m in Case 1 and as large as 200 mV/m in Cases 2 and 3 result from the divergence of the electron pressure gradient (Chanteur, 2000, ch. 14), in Case 1 mainly in the y direction perpendicular to the neutral sheet (inertial field components are much less also here). This shows that, when electrons are decoupled from ions, in fact, electron physics should play a major role in reconnection site.

The sum of these contributions \mathbf{E}_{tot} , equation (1), is displayed in panel n, which is attributed to anomalous (residual) $\eta \mathbf{j}$ electric field. The electromagnetic energy density (power $W \sim \mathbf{j} \cdot \mathbf{E}$) converted to plasma energy from these terms is shown in the panel o, together with the parameter $r_e \equiv |\mathbf{E}_p|/|\mathbf{E}' + \mathbf{E}_a|$, which we conclude is the signature of entering close to the electron dissipation (EDR) reconnection site. In fact, as seen in the last panel p, this value becomes large already in Case 1 (of 10–15) and substantially increases (2 orders of magnitude) when approaching the X line where reconnection takes place.

5. Conclusions

Following the observations of reconnection at the magnetopause and the first crossing of an EDR in the magnetotail by *MMS* on 11 July 2017 reported by Torbert et al. (2018), we have studied three new *MMS* events on the nightside magnetosphere near and at current sheets on 23 and 24 July 2018. The observed magnetic field reversal on current sheet approach is followed by an ion flow reversal but with large fluctuations in the electron velocity. Compared with the temperature asymmetry observed in the EDR of July 2017, during these approaches to the neutral sheet charged particles all exhibit some heating up to energies of a few tens kiloelectron volts for ions and 1–10 keV for electrons and with rather isotropic ion (3–6 keV) and electron temperatures (2–3 keV).

In addition to ideal electric fields, our cases exhibit large (magnitudes of about 1 mV/m) electric fields related to the Hall current, which together with the rather moderate inertial accelerating fields (of 1–2 mV/m), are responsible for the fast reconnection in the IDR. However, during approaches to the EDR, as indicated by a newly devised reconnection parameter, the electric fields arising from the divergence of the full electron pressure tensor provide the main contribution, as large as 20–200 mV/m, to the generalized Ohm's law. We can hence expect that when ions decouple, the electron kinetic physics should provide the mechanism responsible for reconnection processes.

The results obtained here within the *MMS* mission may also be useful for better understanding of the physical mechanisms governing reconnection in various laboratory and astrophysical plasmas.

References

- Baumjohann, W., & Treumann, R. A. (1996). *Basic space plasma physics*. London: Imperial College Press. <https://doi.org/10.1142/p015>
- Biskamp, D. (2000). *Magnetic reconnection in plasmas* (Vol. 3). Cambridge, UK: Cambridge University Press.
- Bruno, R., & Carbone, V. (2016). *Turbulence in the solar wind*, vol. 928. Berlin: Springer International Publishing. <https://doi.org/10.1007/978-3-319-43440-7>
- Burch, J. L., Moore, T. E., Torbert, R. B., & Giles, B. L. (2016). Magnetospheric Multiscale overview and science objectives. *Space Science Reviews*, 199, 5–21. <https://doi.org/10.1007/s11214-015-0164-9>
- Burch, J. L., Torbert, R. B., Phan, T. D., Chen, L.-J., Moore, T. E., Ergun, R. E., et al. (2016). Electron-scale measurements of magnetic reconnection in space. *Science*, 352, aaf2939. <https://doi.org/10.1126/science.aaf2939>
- Burlaga, L. F. (1995). *Interplanetary magnetohydrodynamics*. New York: Oxford University Press.
- Chanteur, G. (2000). Spatial interpolation for four spacecraft: Theory. In *Analysis methods for multi-spacecraft data* (pp. 349–369). Bern: ISSI/ESA Scientific Reports.
- Daughton, W., Nakamura, T. K. M., Karimabadi, H., Roytershteyn, V., & Loring, B. (2014). Computing the reconnection rate in turbulent kinetic layers by using electron mixing to identify topology. *Physics of Plasmas*, 21(5), 052307. <https://doi.org/10.1063/1.4875730>

Acknowledgments

We are grateful for the dedicated efforts of the entire *MMS* mission team, including development, science operations, and the Science Data Center at the University of Colorado. We especially benefited from the efforts of C. J. Pollock and C. T. Russell and the magnetometer team for providing the magnetic field data, available online (<http://cdaweb.gsfc.nasa.gov>). We acknowledge T. E. Moore, Project Scientist, and M. L. Adrian, Deputy Project Scientist, for discussions on the field and plasma instruments. This work has been supported by the *MMS* project through the Catholic University of America during a visit by W. M. Macek to the NASA Goddard Space Flight Center.

- Figura, P., & Macek, W. M. (2013). Model of line preserving field line motions using Euler potentials. *Annals of Physics*, 333, 127–135. <https://doi.org/10.1016/j.aop.2013.03.004>
- Gurnett, D. A., & Bhattacharjee, A. (2005). *Introduction to plasma physics with space and laboratory applications*. Cambridge, UK: Cambridge University Press.
- Krall, N. A., & Trivelpiece, A. W. (1973). *Principles of plasma physics*. New York: McGraw-Hill Book Co.
- Landau, L. D., Lifshitz, E. M., & Pitaevskii, L. P. (1984). *Electrodynamics of continuous media* (Vol. 8). Oxford: Pergamon Press.
- Lazarian, A., Eyink, G., Vishniac, E., & Kowal, G. (2015). Turbulent reconnection and its implications. *Philosophical Transactions of the Royal Society A*, 373, 20140144. <https://doi.org/10.1098/rsta.2014.0144>
- Liu, H., Zong, Q.-G., Zhang, H., Xiao, C. J., Shi, Q. Q., Yao, S. T., et al. (2019). MMS observations of electron scale magnetic cavity embedded in proton scale magnetic cavity. *Nature Communications*, 10(1), 1040. <https://doi.org/10.1038/s41467-019-08971-y>
- Macek, W. M., Krasnińska, A., Silveira, M. V. D., Sibeck, D. G., Wawrzaszek, A., Burch, J. L., & Russell, C. T. (2018). Magnetospheric Multiscale observations of turbulence in the magnetosheath on kinetic scales. *The Astrophysical Journal Letters*, 864(2), L29. <https://doi.org/10.3847/2041-8213/aad9a8>
- Nakamura, T. K. M., Genestreti, K. J., Liu, Y.-H., Nakamura, R., Teh, W.-L., Hasegawa, H., et al. (2018). Measurement of the magnetic reconnection rate in the Earth's magnetotail. *Journal of Geophysical Research: Space Physics*, 123, 9150–9168. <https://doi.org/10.1029/2018JA025713>
- Oieroset, M., Phan, T. D., Haggerty, C., Shay, M. A., Eastwood, J. P., Gershman, D. J., et al. (2016). MMS observations of large guide field symmetric reconnection between colliding reconnection jets at the center of a magnetic flux rope at the magnetopause. *Geophysical Research Letters*, 43, 5536–5544. <https://doi.org/10.1002/2016GL069166>
- Pollock, C., Moore, T., Jacques, A., Burch, J., Gliese, U., Saito, Y., et al. (2016). Fast plasma investigation for Magnetospheric Multiscale. *Space Science Reviews*, 199(1), 331–406. <https://doi.org/10.1007/s11214-016-0245-4>
- Rossi, B., & Olbert, S. (1970). *Introduction to the physics of space*. New York: McGraw-Hill.
- Russell, C. T., Anderson, B. J., Baumjohann, W., Bromund, K. R., Dearborn, D., Fischer, D., et al. (2016). The Magnetospheric Multiscale magnetometers. *Space Science Reviews*, 199, 189–256. <https://doi.org/10.1007/s11214-014-0057-3>
- Spitzer, L. (1956). *Physics of fully ionized gases*. New York: Interscience Publishers.
- Strumik, M., Czechowski, A., Grzedziński, S., Macek, W. M., & Ratkiewicz, R. (2013). Small-scale local phenomena related to the magnetic reconnection and turbulence in the proximity of the heliopause. *The Astrophysical Journal Letters*, 773, L23. <https://doi.org/10.1088/2041-8205/773/2/L23>
- Strumik, M., Grzedziński, S., Czechowski, A., Macek, W. M., & Ratkiewicz, R. (2014). Advective transport of interstellar plasma into the heliosphere across the reconnecting heliopause. *The Astrophysical Journal Letters*, 782, L7. <https://doi.org/10.1088/2041-8205/782/1/L7>
- Torbert, R. B., Burch, J. L., Giles, B. L., Gershman, D., Pollock, C. J., Dorelli, J., et al. (2016). Estimates of terms in Ohm's law during an encounter with an electron diffusion region. *Geophysical Research Letters*, 43, 5918–5925. <https://doi.org/10.1002/2016GL069553>
- Torbert, R. B., Burch, J. L., Phan, T. D., Hesse, M., Argall, M. R., Shuster, J., et al. (2018). Electron-scale dynamics of the diffusion region during symmetric magnetic reconnection in space. *Science*, 362, 1391–1395. <https://doi.org/10.1126/science.aat2998>
- Treumann, R. A. (2009). Fundamentals of collisionless shocks for astrophysical application, 1. Non-relativistic shocks. *Astronomy and Astrophysics Review*, 17, 409–535. <https://doi.org/10.1007/s00159-009-0024-2>
- Treumann, R. A., & Baumjohann, W. (2013). Collisionless magnetic reconnection in space plasmas. *Frontiers in Physics*, 1, 31. <https://doi.org/10.3389/fphy.2013.00031>
- Vasyliunas, V. M. (1975). Theoretical models of magnetic field line merging. *Reviews of Geophysics*, 13, 303–336. <https://doi.org/10.1029/RG013i001p00303>
- Wang, R., Lu, Q., Nakamura, R., Baumjohann, W., Huang, C., Russell, C. T., et al. (2018). An electron-scale current sheet without bursty reconnection signatures observed in the near-Earth tail. *Geophysical Research Letters*, 45, 4542–4549. <https://doi.org/10.1002/2017GL076330>
- Webster, J. M., Burch, J. L., Reiff, P. H., Daou, A. G., Genestreti, K. J., Graham, D. B., et al. (2018). Magnetospheric Multiscale dayside reconnection electron diffusion region events. *Journal of Geophysical Research: Space Physics*, 123, 4858–4878. <https://doi.org/10.1029/2018JA025245>
- Yamada, M., Yoo, J., & Myers, C. E. (2016). Understanding the dynamics and energetics of magnetic reconnection in a laboratory plasma: Review of recent progress on selected fronts. *Physics of Plasmas*, 23(5), 055402. <https://doi.org/10.1063/1.4948721>
- Yordanova, E., Vörös, Z., Varsani, A., Graham, D. B., Norgren, C., Khotyaintsev, Y. V., et al. (2016). Electron scale structures and magnetic reconnection signatures in the turbulent magnetosheath. *Geophysical Research Letters*, 43, 5969–5978. <https://doi.org/10.1002/2016GL069191>